Appl. Phys. A 88, 31–34 (2007)
DOI: 10.1007/s00339-007-3979-8

Applied Physics A
Materials Science & Processing

A. RAHM[1,✉]
M. LORENZ[1]
T. NOBIS[1]
G. ZIMMERMANN[1]
M. GRUNDMANN[1]
B. FUHRMANN[2]
F. SYROWATKA[2]

Pulsed-laser deposition and characterization of ZnO nanowires with regular lateral arrangement

[1] Universität Leipzig, Institut für Experimentelle Physik II, Linnéstr. 5, 04103 Leipzig, Germany
[2] Martin-Luther-Universität Halle-Wittenberg, Interdisziplinäres Zentrum für Materialwissenschaften, Hoher Weg 8, 06120 Halle (Saale), Germany

Received: 28 September 2005/Accepted: 13 January 2007
Published online: 18 April 2007 •

ABSTRACT We report on the high-pressure pulsed-laser deposition growth of periodic arrays of free-standing single zinc oxide nanowires with uniform hexagonal arrangement and cross-section with thickness of less than 100 nm. In order to achieve the wire alignment, we prepared an ordered array of catalytic gold seed particles by a nanosphere lithography mask transfer technique using monodisperse spherical polystyrol nanoparticles. These templates were investigated by scanning electron microscopy and atomic force microscopy prior to nanowire growth. X-ray diffraction revealed the epitaxial relationships between the nanostructures and the *a*-plane sapphire substrate and excellent crystal quality. The optical properties of the ZnO nanowire arrays were measured by cathodoluminescence.

PACS 61.82.Rx; 81.05.-t; 81.05.Dz; 81.10.-h

1 Introduction

Nanoscale one-dimensional zinc oxide (ZnO) structures have stimulated great interest in recent years because of valuable properties such as extraordinary structural diversity [1], radiation hardness, biocompatibility and a high exciton binding energy of 60 meV. Alloying ZnO with Cd and Mg enables band-gap engineering [2] and nanorod quantum-well structures [3]. Furthermore, incorporation of 3d transition metals can produce ferromagnetism in ZnO above room temperature [4]. Nanodimensional device prototypes have already been demonstrated and include nanoscale lasers [5], nanocantilevers [6] and nanowire-field effect transistors [7]. However, a properly defined regular lateral alignment of zinc oxide nanostructures is necessary in order to pave the way to practical applications which are compatible with other technologies. Vertically aligned growth of ZnO nanowires has been successfully achieved based on a gold catalyst driven vapor–liquid–solid (VLS) mechanism on *a*-plane sapphire [8, 9]. Hence, the position of the nanostructures can be pre-determined by the catalyst pattern on the substrate prior to growth. Several such attempts have been made including nano-manipulation of aerosol particles [10] or thermal evaporation through gold nanohole membranes [11] or nanochannel alumina templates [12]. Furthermore, several groups reported the use of self-assembled monolayers of submicron spheres, so-called nanosphere lithography (NSL), for the prepatterning of substrates by a growth catalyst [13, 14].

This technique has been proven to be suitable for the production of arrays of periodically aligned ZnO nanorods [15]. The large area order can facilitate the production of photonic crystals [16]. We report here on the growth of ZnO nanowire arrays by high-pressure pulsed laser deposition (PLD) with uniform hexagonal arrangement of the freestanding single wires. In our work, we use NSL in combination with a mask transfer technique according to Burmeister et al. [17].

2 Experimental details

2.1 *High-pressure PLD technique*

Our samples have been synthesized on $10 \times 10\,\mathrm{mm}^2$ *a*-plane sapphire substrates by a high-pressure PLD process which is especially designed for nanostructure growth [18]. We applied gold as a catalyst according to Sect. 2.2 prior to growth. The target-to-substrate distance was 35 mm. 2000–12 000 pulses of a KrF excimer laser were used to ablate the target with a laser energy density of about $2\,\mathrm{J/cm}^2$. The growth temperature varied between 780 and 830 °C. We used a rotating ZnO target made from pressed and sintered 5N ZnO powder [2]. Argon is used as carrier gas at a background pressure between 50 and 500 mbar and a constant flow between 50 and 500 sccm.

2.2 *Nanosphere lithography*

A scheme of the NSL method can be seen in Fig. 1. For all experiments ultrapure water (Millipore, Simplicity) was used. Monodisperse polystyrene particles (PS, diameter 288 nm or 488 nm, polydispersion index 0.11), received from Microparticles as a 10% suspension in water were further diluted with methanol containing 0.25% Triton X100. $24 \times 24\,\mathrm{mm}^2$ glass substrates were cleaned in 5 : 1 : 1 water/NH_4OH(25%)/H_2O_2(32%) at 80 °C for 15 min and stored in water until used. *a*-plane sapphire (CrysTec) substrates were used as received. The PS particle suspension was spin-coated [19] onto the glass substrate at a speed set to a value between 500 and 1000 rpm. In this case, monolayers as well as bilayers are formed on the glass substrate.

✉ Fax: +49 341 9732668, E-mail: andreas.rahm@physik.uni-leipzig.de

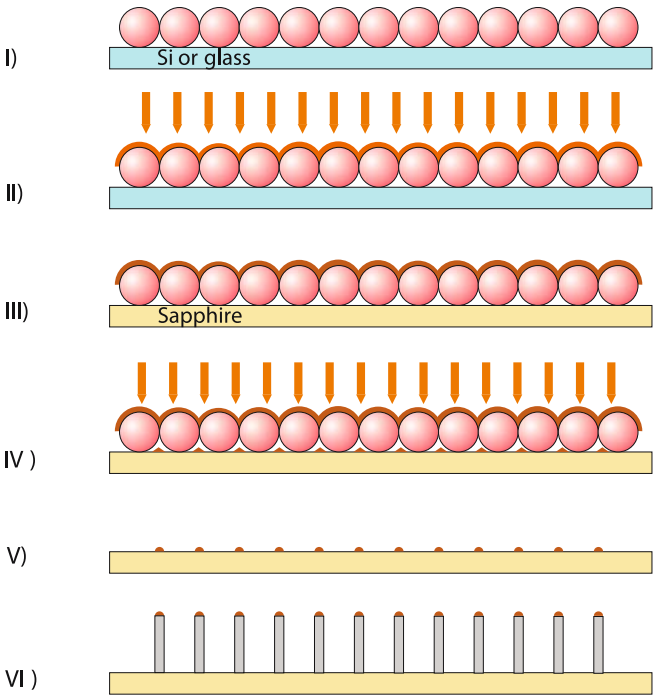

FIGURE 1 Steps of the ZnO nanowire fabrication by NSL, mask transfer and PLD: (I) deposition of polystyrene particle mask on a hydrophilic substrate e.g., Si or glass; (II) deposition of a 60 nm gold layer for mask stabilization by thermal evaporation in high vacuum; (III) transfer of the stabilized mask to the sapphire substrate; (IV) gold deposition by thermal evaporation through the transferred particle mask; (V) sapphire template with ordered gold cluster array after removal of the mask and thermal annealing; (VI) growth of ordered ZnO nanowires by PLD

Then a gold layer of 50 to 70 nm was deposited in a thermal evaporation system (B30.2 HVT, Dresden) on top of the sphere mask for their stabilization at a rate of typical 0.1 to 0.5 nm/s. Thickness of the layers was monitored with a quartz microbalance (MTM20, Gressington). For the mask transfer, the glass substrates were slowly immersed into water at an angle of 30° whereby the Au stabilized mask remained at the water surface and could be transferred to the sapphire substrate. After this, gold was deposited through the mask. After removal of the mask with CH_2Cl_2 in an ultrasonic bath for 2 min, regular arrays of gold particles remained on the sapphire surface.

2.3 *Characterization*

The topography of the prestructured substrates was characterized by a Vecco Metrology Dimension 3100/Nanoscope IV atomic force microscope (AFM). We used standard Si cantilevers in the tapping mode at a frequency of 300 kHz. Scanning electron microscopy images were recorded prior and after the PLD growth process using a XL30 FEG environmental scanning electron microscope (ESEM) by FEI in high-vacuum mode. The epitaxial relations were revealed by X-ray diffraction (XRD) with a Philips XPert with two goniometers, one with crossed slit collimators for recording wide-angle diffractograms and one equipped with a Bonse–Hart collimator (high-resolution (HR-XRD) using Cu $K_{\alpha 1}$ radiation. The optical properties of the as-grown ZnO nanowire arrays were investigated by room-temperature cathodoluminescence spectroscopy (CL) with a Yobin Yvon multichannel CCD detector.

3 Results and discussion

In Fig. 2a an ESEM picture with ordered gold seeds, which were obtained from gold evaporation through a transferred mask, can be seen. The corresponding polystyrene particle (488 nm) mask for NSL which was stabilized with 60 nm Au is shown in the inset. The ordered array of gold particles on sapphire exhibits some defects (Fig. 2b). However, the periodicity within one domain is perfect as indicated by the line scan in Fig. 2c. We observed for the spheres with 287 nm diameter a smaller long-range order than for the 488 nm polystyrene spheres. By tuning the parameters of the NSL process, we could also achieve masks with double and triple layers of polystyrene particles. The ESEM images in Fig. 3 present typical examples of ZnO nanowire arrays obtained from high-pressure PLD growth on prestructured substrates. These nanowires exhibit a length of about 1 μm and are aligned perpendicular to the substrate surface. The structures have a hexagonal cross section (see Fig. 3a) and diameter ranges from 60 nm (2000 laser pulses) up to 150 nm (12 000 laser pulses). It can be seen that the lateral arrangement of the columnar structures resembles closely the hexagonal patterning of the catalyst. The nanowire samples prepared with the mask transfer technique (Fig. 3b) had a better long-range order with larger domains compared to samples where the mask was directly arranged on the sapphire substrate (Fig. 3a). We have varied the thickness of the catalytic particles between 4 and 21 nm. This difference had no influence on the nanowire diameter. However, without the mask transfer technique and for gold seed thickness above 15 nm we observed unordered growth in the regions formerly covered by monolayers of mask spheres. Periodic ordering was present in regions which were covered originally by a triple (ABA) polystyrene sphere layer (Fig. 3a). We attribute this to the presence of gold a little bit below the spheres and the formation of several gold droplets at the growth temperature which can be avoided by either reducing the hole size in the polystyrene sphere mask (i.e., using the mask transfer technique) or by evaporating less gold through the mask. In the ordered regions there was always one whisker per seed catalytic particle as expected in the VLS growth model.

In the wide-angle diffractogram (Fig. 4) of the sample shown in Fig. 3b, only the ZnO(000l) reflections and the peaks from the *a*-plane sapphire substrate are visible. Therefore, the ZnO whiskers grow along their *c*-axis perpendicular to the substrate. *φ*-scans (not shown) of the ZnO$\{11\bar{2}4\}$ reflections and the $Al_2O_3\{22\bar{4}6\}$ reveal the following in-plane epitaxial relationship: ZnO$\langle 11\bar{2}0\rangle \parallel [0001]Al_2O_3$. We observed no rotation domains. The FWHM$(2\theta-\omega)$ of the HRXRD (0002) reflection of ZnO varied between 54 and 105 arcsec and the rocking curve width (inset in Fig. 4) was typically 0.15° which is comparable to the best values reported for ZnO PLD thin films and nanowires [2, 20, 21]. From HRXRD reciprocal space maps [22], we determined the *c*-axis lattice constant to be 5.207 ± 0.001 Å and the *a*-axis lattice constant to be 3.25 ± 0.01 Å, which is exactly the zinc oxide bulk value. Therefore, we conclude that our structures grow fully relaxed.

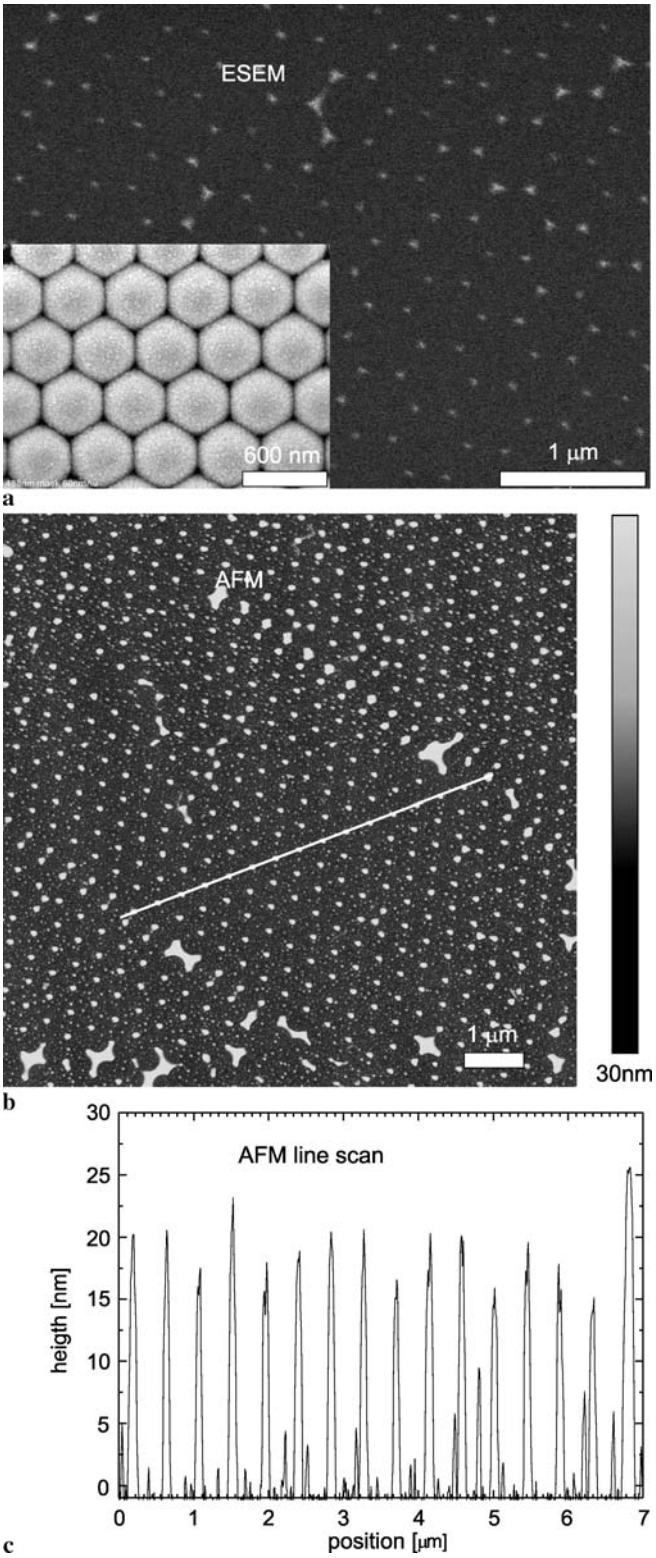

FIGURE 2 (**a**) Gold seeds on sapphire obtained by the mask transfer technique; *inset*: stabilized polystyrene sphere mask (488 nm). (**b**) AFM image of the sapphire substrate with hexagonally ordered gold droplets. (**c**) AFM line scan as indicated in (**b**) by *white solid line*

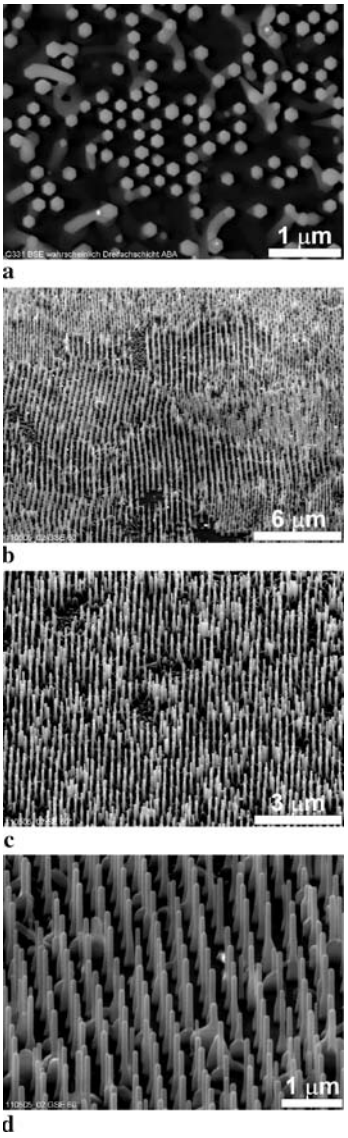

FIGURE 3 ESEM pictures of as-grown samples. (**a**) Without mask transfer technique; a triple ABA nanospheres (287 nm) layer was used. (**b**–**d**) Different magnifications of a sample prepared by mask transfer technique (488 nm PS spheres)

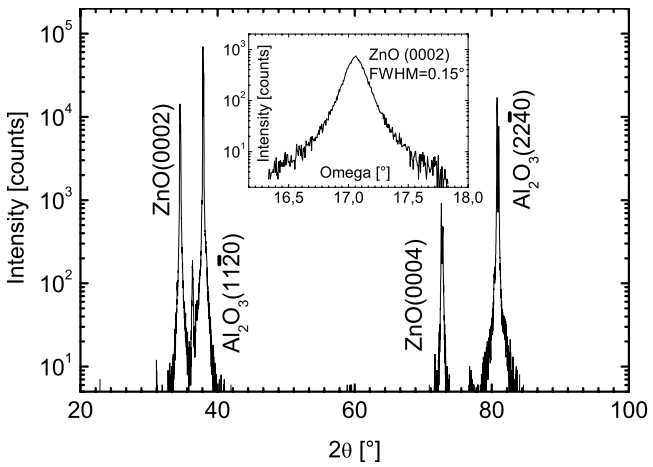

FIGURE 4 X-ray 2θ–ω-scan of an ordered ZnO nanowire array showing only the ZnO(000l) and the substrate reflection. The HRXRD rocking curve of the ZnO(0002) peak is shown in the *inset*. The analyzed area was several mm^2

Figure 5 depicts CL measurements at two different sample positions. The ZnO nanowires show two luminescence bands, the first around 3.25 eV (ultraviolet emission, UV range), the second around 2.35 eV (green or visible emission, VIS range).

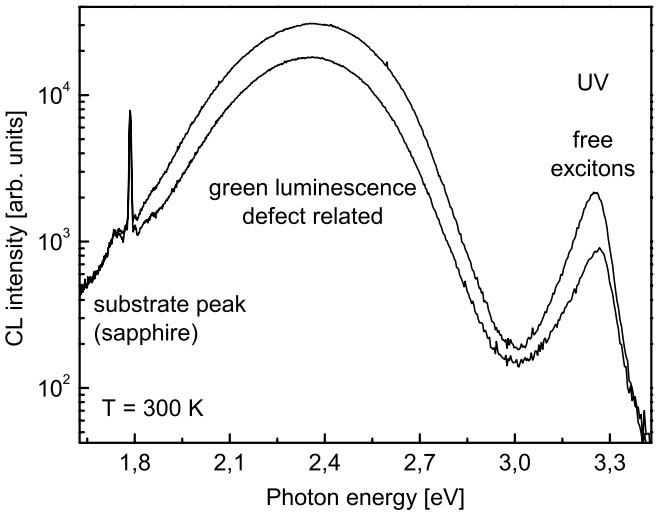

FIGURE 5 Cathodoluminescence spectra of an array of ordered nanowires at room temperature. The two *curves* represent different sample positions

While the first emission is associated with exciton emission, the second usually indicates recombination at deep levels, presumably caused by oxygen defects [23]. These optical features correspond to the standard ZnO emission spectrum and no additional features due to the ordering of the nanocrystals is observed.

4 Conclusion

We have reproducibly prepared periodically arranged gold seeds on sapphire substrates by a nanosphere lithography mask transfer technique. Based on these catalytic particles, we have successfully grown hexagonally arranged zinc oxide nanowires with hexagonal cross section by high-pressure PLD. We have shown that the mask transfer step in the NSL process improves the long-range order. The epitaxial growth of vertically aligned nanocolumns was achieved with excellent crystalline quality. We propose that these ordered nanostructure arrays may form the basis for novel nanooptical devices based on ZnO.

ACKNOWLEDGEMENTS This work was supported by the DFG within FOR 522 (Gr 1011/11-1).

REFERENCES

1 Z.L. Wang, J. Phys. C Condens. Matter **16**, R829 (2004)
2 M. Lorenz, E.M. Kaidashev, H. von Wenckstern, V. Riede, C. Bundesmann, D. Spemann, G. Benndorf, H. Hochmuth, A. Rahm, H.-C. Semmelhack, M. Grundmann, Solid State Electron. **47**, 2205 (2003)
3 T. Yatsui, J. Lim, M. Ohtsu, S.J. An, G.-C. Yi, Appl. Phys. Lett. **85**, 727 (2004)
4 M. Diaconu, A. Pöppl, R. Böttcher, J. Hoentsch, A. Klunker, D. Spemann, H. Hochmuth, M. Lorenz, M. Grundmann, Phys. Rev. B **72**, 085 214 (2005)
5 J.C. Johnson, H. Yan, R.D. Schaller, L.H. Haber, R.J. Saykally, P. Yang, J. Phys. Chem. B **105**, 11 387 (2001)
6 W.L. Hughes, Z.L. Wang, Appl. Phys. Lett. **82**, 2886 (2003)
7 M.S. Arnold, P. Avouris, Z.W. Pan, Z.L. Wang, J. Phys. Chem. B **107**, 659 (2003)
8 A.P. Levitt (Ed.), *Whisker Technology* (Wiley-Interscience, New York, 1970)
9 M. Lorenz, E.M. Kaidashev, A. Rahm, T. Nobis, J. Lenzner, G. Wagner, D. Spemann, H. Hochmuth, M. Grundmann, Appl. Phys. Lett. **86**, 143 113 (2005)
10 B.J. Ohlsson, M.T. Björk, M.H. Magnusson, K. Deppert, L. Samuelson, L.R. Wallenberg, Appl. Phys. Lett. **79**, 3335 (2001)
11 H.J. Fan, F. Fleischer, W. Lee, K. Nielsch, R. Scholz, M. Zacharias, U. Gösele, A. Dadgar, A. Krost, Superlattices Microstruct. **36**, 95 (2004)
12 Z.H. Wu, X.Y. Mei, D. Kim, M. Blumin, H.E. Ruda, Appl. Phys. Lett. **81**, 5177 (2002)
13 X. Wang, C.J. Summers, Z.L. Wang, Nano Lett. **4**, 423 (2004)
14 D. Banerjee, J. Rybczynski, J.Y. Huang, D.Z. Wang, K. Kempa, Z.F. Ren, Appl. Phys. A **80**, 749 (2005)
15 J. Rybczynski, D. Banerjee, A. Kosiorek, M. Giersig, Z.F. Ren, Nano Lett. **4**, 2037 (2004)
16 K. Kempa, B. Kimball, J. Rybczynski, Z.P. Huang, P.F. Wu, D. Steeves, M. Sennett, M. Giersig, D.V.G.L.N. Rao, D.L. Carnahan, D.Z. Wang, J.Y. Lao, W.Z. Li, Z.F. Ren, Nano Lett. **3**, 13 (2003)
17 F. Burmeister, C. Schafle, T. Matthes, M. Bohmisch, J. Boneberg, P. Leiderer, Langmuir **13**, 2983 (1997)
18 M. Lorenz, E.M. Kaidashev, A. Rahm, T. Nobis, J. Lenzner, G. Wagner, D. Spemann, H. Hochmuth, M. Grundmann, Appl. Phys. Lett. **86**, 143 113 (2005)
19 J.C. Hulteen, R.P. Van Duyne, J. Vac. Sci. Technol. A **13**, 1553 (1995)
20 A. Ohtomo, M. Kawasaki, T. Koida, K. Masubuchi, H. Koinuma, Y. Sakurai, Y. Yoshida, T. Yasuda, Y. Segawa, Appl. Phys. Lett. **72**, 2466 (1998)
21 S. Choopun, R.D. Vispute, W. Yang, R.P. Sharma, T. Venkatesan, H. Shen, Appl. Phys. Lett. **80**, 1529 (2002)
22 P.F. Fewster, *X-ray Scattering from Semiconductors* (Imperial College Press, London, 2000)
23 B. Lin, Z. Fu, J. Jia, Appl. Phys. Lett. **79**, 943 (2001)